Long-term measurements of chlorophyll *a* fluorescence using the JIP-test show that combined abiotic stresses influence the photosynthetic performance of the perennial ryegrass (*Lolium perenne*) in a managed temperate grassland

Anthony Digrado[a], Aurélie Bachy[b], Ahsan Mozaffar[b,c], Niels Schoon[c], Filippo Bussotti[d], Crist Amelynck[c,e], Anne-Catherine Dalcq[f], Marie-Laure Fauconnier[g], Marc Aubinet[b], Bernard Heinesch[b], Patrick du Jardin[a] and Pierre Delaplace[a,*]

[a]Plant Biology Laboratory, AGRO-BIO-CHEM, University of Liège-Gembloux Agro-Bio Tech, 5030 Gembloux, Belgium

[b]Biosystems Dynamics and Exchanges, TERRA, University of Liège-Gembloux Agro-Bio Tech, 5030 Gembloux, Belgium

[c]Royal Belgian Institute for Space Aeronomy, Uccle, 1180, Belgium

[d]Department of Agri-Food Production and Environmental Science, University of Florence, 50144 Florence, Italy

[e]Department of Analytical Chemistry, Ghent University, 9000 Ghent, Belgium

[f]Modeling and development Unit, AGRO-BIO-CHEM, University of Liège-Gembloux Agro-Bio Tech, 5030 Gembloux, Belgium

[g]Agro-Bio Systems Chemistry, TERRA, University of Liège-Gembloux Agro-Bio Tech, 5030 Gembloux, Belgium

*Corresponding author, e-mail: pierre.delaplace@ulg.ac.be

Several experiments have highlighted the complexity of stress interactions involved in plant response. The impact in field conditions of combined environmental constraints on the mechanisms involved in plant photosynthetic response, however, remains understudied. In a long-term field study performed in a managed grassland, we investigated the photosynthetic apparatus response of the perennial ryegrass (*Lolium perenne*) to environmental constraints and its ability to recover and acclimatize. Frequent field measurements of chlorophyll *a* fluorescence (ChlF) were made in order to determine the photosynthetic performance response of a population of *L. perenne*. Strong midday declines in the maximum quantum yield of primary photochemistry (F_V/F_M) were observed in summer, when a combination of heat and high

This article has been accepted for publication and undergone full peer review but has not been through the copyediting, typesetting, pagination and proofreading process, which may lead to differences between this version and the Version of Record. Please cite this article as doi: 10.1111/ppl.12594

light intensity increased photosynthetic inhibition. During this period, increase in photosystem I (PSI) activity efficiency was also recorded, suggesting an increase in the photochemical pathway for de-excitation in summer. Strong climatic events (e.g., heat waves) were shown to reduce electron transport between photosystem II (PSII) and PSI. This reduction might have preserved the PSI from photo-oxidation. Periods of low soil moisture and high levels of sun irradiance increased PSII sensitivity to heat stress, suggesting increased susceptibility to combined environmental constraints. Despite the multiple inhibitions of photosynthetic functionality in summer, the *L. perenne* population showed increased PSII tolerance of environmental stresses in August. This might have been a response to earlier environmental constraints. It could also be linked to the selection and/or emergence of well-adapted individuals.

Abbreviations – ChlF, chlorophyll *a* fluorescence; ΔV_{IP}, efficiency/probability that a photon trapped by the PSII RC moves an electron into the electron transport chain beyond PSI; F_V/F_M, maximum quantum yield of photosystem II; O, J, I, P, intermediate steps at 50 µs, 2 ms, 30 ms and at the maximum of chlorophyll *a* fluorescence; OEC, oxygen evolving complex; PI_{ABS}, performance index on absorption basis; PPFD, photosynthetic photon flux density; PQ, plastoquinone; Ψ_{E0}, efficiency/probability that a photon trapped by the PSII RC moves an electron into the electron transport chain beyond Q_A; PSI, photosystem I; PSII, photosystem II; Q_A, primary electron acceptor quinone of PSII; Q_B, secondary electron acceptor quinone of PSII; RC, reaction center; VPD, vapor pressure deficit.

Introduction

Many studies have evaluated plant responses to environmental stresses and have reported effects on the photosynthetic process (Georgieva et al. 2000, Hassan 2006, Mathur et al. 2011, Bussotti et al. 2014). For instance, high temperature has been shown to be particularly detrimental, with several studies reporting that photosynthesis is one of the most heat-sensitive processes in plants (Luo et al. 2011, Yan et al. 2012, Guidi and Calatayud 2014). High temperatures are also known to cause a loss of the manganese cluster functionality in photosystem II (PSII), which leads to the inhibition of the oxygen evolving complex (OEC) component (Nash et al. 1985, Tóth et al. 2007b, Oukarroum et al. 2009). This impairment of photosynthetic activity has been shown to affect CO2 fixation (Guidi and Calatayud 2014). Under drought stress conditions, studies have also reported a decrease in the CO2 assimilation rate due to a decrease in stomatal conductance (Cruz de Carvalho et al. 2010, Rahbarian et al. 2011). High ozone concentrations can also induce a depression in net photosynthesis (Bussotti et al. 2007, Cascio et al. 2010) and the inactivation of the end acceptors of electrons by oxidative damage of the cellular content has been reported in numerous studies (Desotgiu et al. 2010, Bussotti et al. 2011).

The photosynthetic apparatus, however, is able to trigger protective mechanisms under stressful environments favoring acclimatization (for definition, see Wilson and Franklin 2002). For instance, plants

can promote an increase in energy dissipation within the light harvesting complex in order to reduce PSII excitation when submitted to high irradiance (Jahns and Holzwarth 2012, Goh et al. 2012) or to adjust the electron transport rate within the PSII reaction center (RC) (Derks et al. 2015). Usually, however, plants encounter combined environmental stresses in natural conditions. Two stresses sometimes require antagonistic responses, such as drought and heat stress which lead to the opening or closure of stomata in *Arabidopsis*, respectively (Rizhsky et al. 2002, Mittler 2006). This makes it difficult to predict plant response to combined environmental constraints. Some studies have shown increased PSII thermotolerance under drought conditions (Oukarroum et al. 2009, Snider et al. 2013), whereas others have shown increased PSII sensitivity to heat (Jiang and Huang 2001, Tozzi et al. 2013). The combination of high temperatures with high levels of light has also been shown to promote PSII inhibition (Janka et al. 2015), whereas some studies have found that high levels of light could promote PSII thermotolerance (Georgieva et al. 2003). These examples highlight the complexity of stress interaction and the need for further studies on the mechanisms involved in plant photosynthetic response to combined environmental constraints.

Analyses of chlorophyll *a* fluorescence (ChlF) have been used in several studies to investigate the physiological aspects of photosynthesis. Fast fluorescence transients measured by a plant efficiency analyzer (PEA) and modulated fluorescence signals obtained from a pulse-amplitude modulated (PAM) fluorimeter both provide parameters that describe photosynthesis functionality and are widely used. Measurements conducted with a PAM fluorimeter use light-adapted leaves, whereas fast fluorescent transients are derived from dark-adapted leaves. This implies that measurements in dark-adapted conditions give information on the 'potential' photosynthetic performance rather than the actual photosynthetic efficiency. PEA fluorimeter enables to acquire lot of data in a short period of time, making monitoring and large-scale surveys possible. The fast fluorescent transients can be analyzed using the JIP-test, which provides useful information on the status and functioning of the photosynthetic apparatus (Maxwell and Johnson 2000, Kalaji et al. 2016). When plotted on a logarithmic scale, the fluorescence transients exhibit a polyphasic rise called the OJIP curve (referring to the O, J, I, P steps at 50 μs, 2 ms, 30 ms and maximum ChlF yield). The rise in ChlF emission from its basal level (= O step) reflects the gradual accumulation of Q_A in its reduced form. The O–J phase of the curve is related to single turnover events (i.e., Q_A is reduced only once) of the primary reactions of photochemistry and represents the reduction of the acceptor side of PSII (Oukarroum et al. 2007). The J phase is influenced by the rate limitation caused by the reduction of the plastoquinone (PQ) pool (Tóth et al. 2007a). The J–I phase of the curve is therefore representative of the reduction/oxidation of the PQ pool. The last and slowest phase in the rise in ChlF emission, the I–P phase, is related to electron transfer through PSI and is attributed to the reduction of the acceptor side of the PSI (Schansker and Strasser 2005). It has been demonstrated that the

shape of the OIJP curve is related to the physiological status of plants (Strasser et al. 2000). The parameters determined with the JIP-test therefore provide a very useful tool for investigating the response and adaptive ability of the photosynthetic apparatus to a wide range of stressors (Bussotti et al. 2007, 2010, Redillas et al. 2011, Brestic et al. 2012).

Among the various cultivated agro-systems, grasslands represent ~26% of the terrestrial surface (Brunner et al. 2007, Boval and Dixon 2012) and about 80% of agricultural land (Boval and Dixon 2012). Grasslands play a significant role in carbon sequestration (Boval and Dixon 2012, Chang et al. 2015) and water catchments, and are a reserve of biodiversity (Boval and Dixon 2012). A good understanding of the health status of these ecosystems is therefore a key issue if one wants to preserve or increase these ecosystem services under current and future climatic conditions. For these reasons, we decided to investigate the photosynthetic response to the naturally co-occurring environmental constraints of the perennial ryegrass (*Lolium perenne*), an important grassland species, over 2 successive years using the JIP-test. We sought to answer the following questions: (i) How does the photosynthetic apparatus respond to combined environmental constraints and which mechanisms of photosynthetic processes are involved? (ii) What is the recovery capacity of photosynthetic performance after repeated stressful events? (iii) Is there any evidence of photosynthetic acclimatization? We hypothesize that the greatest decline in photosynthetic performance will occur when environmental stresses are combined because of potential synergistic interactions. A succession of unfavorable events might also lead to the potential acclimatization in *L. perenne* population.

Materials and methods

Field site

The study was carried out within the framework of the CROSTVOC project (CROp Stress Volatile Organic Compounds: CROSTVOC 2015). All measurements were performed at the Dorinne Terrestrial Observatory (DTO) (Fig. S1) in Belgium (50°18'44'' N and 4°58'07'' E). The climate at this site is temperate oceanic. The site area is a permanent grassland covering 4.22 ha, and the relief is dominated by a large colluvial depression oriented south-west/north-east. This depression lies on a loamy plateau with a calcareous and/or clay substrate. Altitudes range from 240 m (north-east) to 272 m (south). The paddock had been converted to permanent grassland at least 50 years before the start of this study and has been intensively grazed by cattle, with the application of cattle slurry and manure. The botanical diversity was evaluated on 24 quadrats (0.5 × 0.5 m) in September 2010 and June 2011. The plant communities were composed of 13 grass species (*Agrostis stolonifera*, *Alopecurus geniculatus*, *Bromus hordeaceus*, *Cynosurus cristatus*, *Dactylis glomerata*, *Elymus repens* (L.) Gould, *Festuca pratensis* Huds., *Holcus lanatus*, *Lolium multiflorum* Lam., *L. perenne*, *Poa annua*, *Poa pratensis* and *Poa trivialis*), one nitrogen

(N)-fixing dicot (*Trifolium repens*) and seven non-N-fixing dicots (*Capsella bursa-pastoris* (L.) Medik., *Carduus*, *Matricaria discoidea* DC., *Plantago major*, *Ranunculus repens*, *Stellaria media* (L.) Vill. and *Taraxacum* sp.). The perennial ryegrass *L. perenne* was the main and most representative species in the grassland, being present in every quadrat and in the greatest relative abundance (based on the surface occupation) in the quadrats (Table S1).

Micro-meteorological data

Micro-meteorological data such as photosynthetic photon flux density (SKP215, Skye Instruments, Llandrindod Wells, UK), air temperature and air relative humidity (RHT2nl, Delta-T Devices Ltd, Burwell, Cambridge, UK) at 2.62 m above soil level, as well as ozone concentration (T400, Teledyne, San Diego, CA) at 1 m above soil level, and soil moisture (CS616, Campbell Scientific Inc., Logan, UT) and soil temperature (PT 1000, Campbell Scientific Inc., Logan, UT) at a depth of 5 cm were recorded every 30 min in the grassland during the measurement periods using the aforementioned equipment. The vapour pressure deficit (VPD) was calculated from the temperature and relative humidity measurements.

Analysis of the fluorescence transient using the JIP-test

Measurements of the ChlF emissions of *L. perenne* were conducted at the DTO on three plots (each 30 × 5 m) from June to October 2014 and from May to October 2015, using a HandyPEA fluorimeter (Hansatech Instruments, Pentney, Norfolk, UK). Cows were allowed to graze on days when no measurements were being taken. Measurements were performed in each monitored plot four times a day at 11:00, 13:00, 15:00 and 17:00 h (local time zone). The number of replicates for each plot and time period was 7 in 2014 and 8 in 2015. In addition, on 31 July 2015 and 13 August 2015, when there were contrasting micro-meteorological conditions, the full diurnal evolution of ChlF was investigated by taking measurements every 2 h from pre-dawn (5:00) till evening (19:00) on the three plots, giving eight sample time periods rather than four. Measurements were performed on non-senescent mature leaves. Prior to each measurement, leaves were dark-adapted with leaf clips for 30 min. The leaf clips were adapted to the width of the *L. perenne* leaves by reducing by half the measurement surface with a black vinyl electrical tape, following the manufacturer's recommendations. The surfaces of the dark-adapted leaves were then exposed for 1 s to red light with a flux density of 3000 μmol m^{-2} s^{-1} provided by an array of three light-emitting diodes (peak wavelength at 650 nm). After irradiance of the sample, the induced subsequent fluorescence signals were recorded every 10 μs from 10 to 300 μs, then every 100 μs till 3 ms, then every 1 ms till 30 ms, then every 10 ms till 300 ms and finally every 100 ms till 1 s.

Fluorescence emissions measured at 50 μs (F_{50}, step O), 300 μs (F_{300}, step K), 2 ms (step J), 30 ms (step I) and maximum yield (F_M, step P) were used to determine several parameters describing photosynthesis activity according to the JIP test (Strasser et al. 2000, 2004). These parameters are

summarized in Table 1. When a ChlF parameter showed an aberrant value (i.e., infinite), all parameters derived from this specific measurement were discarded (0.06% of the dataset).

Statistical analysis

Three groups of comparable meteorological conditions were defined by clustering (Ward's method based on the Euclidian distance). Clustering was performed on coordinates of the two first principal components of a principal component analysis (PCA). All meteorological parameters were entered as variables in this PCA, apart from ozone concentration. In order to study the influence of monitored plots on ChlF response, a general linear model (GLM) type III was realized, with the meteorological group previously created and the monitored plots as factors. The monitored plots were considered as random factor. As its influence was not found to be significant, the values of ChlF parameters were averaged without consideration of the different plots. Three groups of comparable photosynthetic response based on ChlF measurements were then defined using the same methodological approach as that for the meteorological groups. The averaged ChlF parameter values were entered as variables in the PCA. The Tukey's Honest Significant Difference test (Tukey HSD) was used to classify the mean values of ChlF and the meteorological parameters between the meteorological and ChlF clusters created. When comparing days with contrasting meteorological conditions, the difference in ChlF parameter values between the 2 days was tested using a GLM for each of the eight sample time periods.

The correlations between ChlF and meteorological parameters were tested using a Pearson correlation test. We decided to complement this approach with a canonical correlation analysis (CCA), a multivariate statistical test, to explore the relationship between photosynthetic responses and meteorological conditions and the interdependence within a set of variables. With this method, the first canonical axis is constructed as linear combinations of variables within the sets in order to maximize the correlation between the two datasets (i.e., ChlF and meteorological datasets).

A GLM was used to predict ChlF parameters based on meteorological variables and their second-order interactions. The minimum adequate model for each ChlF parameter was selected using a stepwise algorithm based on the Akaike's information criterion. Only significant interactions were conserved. The total variance explained by the models (R^2) was then decomposed in order to evaluate the relative variance explained by each predictor variable and the various interactions. Linear regression followed by an analysis of covariance (ANCOVA) was used to evaluate the potential modification in the relationship between the ChlF and meteorological parameters for different environments and months. All the operations were performed using Minitab® software version 17.1.0 (State College, Pennsylvania, PE) and R software version 3.3.0 (R Development Core Team 2012), with the following R package: 'FACTOMINER' (Husson et al. 2016), 'VEGAN' (Oksanen et al. 2012), 'CCP' (Menzel 2015), 'CAR' (Fox

et al. 2016) and 'RELAIMPO' (Groemping and Matthias 2013). Square root-transformed values (unless stated otherwise) of the ChlF parameters were used to improve the normality and homogeneity of variances when required by the statistical test.

Results

Environmental conditions

The days of ChlF measurements and their dispersion were representative of the period studied, especially in the second year (Fig. S2). Irradiance reached its highest values from May to August (referred to here as summer) for both years, with midday photosynthetic photon flux density (PPFD) values above 1500 µmol m^{-2} s^{-1} on most of the measured days (Fig. 1A). From September to October (referred to here as autumn), the PPFD values were below that level. From June 30 to July 5, 2015 a heat wave (as defined by D'Ippoliti et al. 2010) hit Belgium and was recorded at the DTO. ChlF measurements during this period were limited to the first and third day of the heat wave, with maximum air temperatures (T) of 28.9 and 33°C recorded during the ChlF measurement (Fig. 1B). In summer, the ozone concentration values (O_3) were above 60 ppbv, whereas it remained below this level in autumn (Fig. 1E). The second year of monitoring was characterized by two dry spells in summer. In June and August, the soil moisture (SM5) was ca. 20% for 2 weeks (Fig. 1C). The highest VPD values were measured from June to August, with values above 2.0 kPa, but in September and October they generally did not exceed 1.0 kPa (Fig. 1D).

Temporal evolution of ChlF emissions

In both years of the study, a seasonal (Fig. 2) and diurnal (Fig. 3) evolution of ChlF parameters was observed in the grassland. The largest diurnal amplitudes of ChlF parameters were detected in summer with variations of 68, 99, 41 and 148% with respect to the initial morning value for the maximum quantum yield of PSII (F_V/F_M), the performance index (PI_{ABS}), the J phase (Ψ_{E0}) and the I–P phase (ΔV_{IP}) respectively. The ChlF parameters showed lower diurnal variation in autumn. The highest F_V/F_M values were measured in autumn, with average basal values of ca. 0.75, indicating high PSII efficiency. In contrast, values as low as 0.15 were measured in summer. The lowest PI_{ABS} values were also measured in summer, indicating a low photosynthetic performance of the *L. perenne* population. PI_{ABS} graphically exhibited an increasing trend at the end of the 2014 growing season. This increase also occurred in the following year, but was less pronounced. The Ψ_{E0} showed a less marked diurnal and seasonal pattern and fluctuated around 0.56, with occasional midday decreases below 0.40 observed in summer, reflecting a decrease in the efficiency of the electron transport beyond Q_A during these periods. The ΔV_{IP} presented stable values around 0.32 in autumn, but several midday peaks above 0.55 were observed in summer, indicating a rapid reduction of the end electron acceptor.

A diurnal decrease in F_V/F_M was observed simultaneously with a decrease in PI_{ABS} and an increase in ΔV_{IP} (Fig. 3). A less pronounced diurnal pattern was observed for Ψ_{E0} (Fig. 3C). The diurnal variation of ChlF parameters was stronger under environmental stress, as described in the next paragraph. There were few perceptible differences in Ψ_{E0} behavior between the two contrasting days (Fig. 3C). Significant differences ($p \leq 0.001$) between these were observed in the morning for all ChlF parameters, with lower F_V/F_M, PI_{ABS} and Ψ_{E0} values and higher ΔV_{IP} values on 31 July 2015 than on 13 August 2015. These differences were not more significant ($p \geq 0.05$) 6 h after sunrise, except for PI_{ABS}. Even when strong diurnal variations of ChlF parameters were measured (e.g., 13 August 2015), the evening values (i.e., 14 h after sunrise) of ChlF parameters were comparable with those measured 6 h after sunrise (i.e., before the onset of strong diurnal variation) and did not differ ($p \geq 0.05$) from evening values measured on a day with lower diurnal variation (Fig. 3).

Impact of environmental conditions on ChlF emissions

The Pearson correlations test (Table 2) showed that F_V/F_M and ΔV_{IP} were the ChlF parameters that were most affected by environmental conditions, correlations being higher than 0.52 in absolute value for six out of seven meteorological parameters. In contrast, Ψ_{E0} correlated poorly with meteorological parameters (all correlation coefficients were below 0.24 in absolute value). The relationship between environmental parameters and the ChlF parameters F_V/F_M and PI_{ABS} differed greatly from that between environmental parameters and the ChlF parameters Ψ_{E0} and ΔV_{IP}. PPFD, T and VDP were the meteorological parameters that had the strongest influence on ChlF parameters, the minimum correlation being above 0.55 in absolute value for F_V/F_M, PI_{ABS} and ΔV_{IP}. In contrast, SM5 was the meteorological parameter with the least influence on ChlF, with no correlation exceeding 0.35 in absolute value. The strong influence of PPFD, T and VPD on ChlF parameters was confirmed by the analysis of the relative contribution of meteorological parameters to ChlF variation (Fig. 4). The analysis also revealed the influence of synergistic interactions between meteorological parameters. Interactions between meteorological parameters had a non-negligible contribution to ChlF variation and explained 22.8, 12.3, 33.0 and 4.9% of the F_V/F_M, PI_{ABS}, Ψ_{E0} and ΔV_{IP} variance respectively. The Ψ_{E0} was the parameter most influenced by meteorological parameters interactions whereas ΔV_{IP} was the least influenced.

Three meteorological clusters were defined using PCA-clustering (Table 3). From the M1 to M3 clusters, environmental conditions were characterized by increasing PPFD, T, VPD and TS5 values and decreasing SM5 and RH values. Whereas M1 conditions were more frequently found in autumn, M3 conditions were more common in summer. Three ChlF clusters were also defined by PCA-clustering (Table 3). The C1 cluster was characterized by high F_V/F_M and PI_{ABS} values, indicating good functionality of the photosynthetic apparatus. A reduction of up to 60% and 93% in average values from the C1 to C3

cluster was observed for F_V/F_M and PI_{ABS}, respectively, indicating a decrease in photosynthetic performance in C3. Ψ_{E0} exhibited lower relative change between clusters and decreased by only 19% from C1 to C3. ΔV_{IP} exhibited a significant +50% increase from C1 to C2. The difference in ΔV_{IP} values between C2 and C3 was not significant. ChlF response characterized by the C3 response was common in summer, whereas the C1 response was common in autumn. CCA revealed that M1 conditions in the grassland could be associated with the ChlF response characterized by the C1 cluster (Fig. 5) and could therefore be qualified as non-stressful conditions. The C3-cluster type of ChlF response was correlated with environmental conditions characterized by the M3 cluster that could therefore be qualified as conditions of strong environmental constraints. M2 conditions in the grassland could be associated to ChlF response characterized by either the C1 or C2 clusters (Fig. 3) and could therefore be qualified as conditions of moderate environmental constraints. Days usually began with meteorological conditions characterized by the M1 cluster and the ChlF response corresponding to the C1 cluster. At midday, meteorological conditions could change to the M2 or M3 clusters and the ChlF response to the C2 or C3 clusters.

The F_V/F_M response to combined stresses received particular attention because it is one of the most studied ChlF parameters and in our study was one of the parameters the most influenced by the combination of meteorological parameters. The linear relationship between F_V/F_M and abiotic stresses varied with environmental conditions (Fig. 6). A stronger decrease in F_V/F_M in relation to air temperature was measured where soil moisture was below 20.5% ($p \leq 0.001$, Fig. 6A). Soil moisture conditions, however, did not have a significant influence on the F_V/F_M response to increasing PPFD ($p \geq 0.05$, Fig. 6B) and increasing VPD ($p \geq 0.05$, Fig. 6C). An altered linear relationship between F_V/F_M and abiotic stresses in the grassland was also observed at different sun irradiance levels. Stronger decreases in F_V/F_M in relation to increasing air temperatures were observed at higher sun irradiance levels ($p \leq 0.001$, Fig. 6D). The F_V/F_M response to VPD did not differ at moderate and high sun irradiance levels (Fig. 6F). The relationship between F_V/F_M and VPD at moderate and high sun irradiance levels, however, could not be compared with the relationship at low irradiance level because no observations at VPD > 2.0 kPa were performed for the latter. Sun irradiance levels in the grassland did not induce a stronger decrease in F_V/F_M in relation to increasing soil moisture (Fig. 6E).

Sensitivity of PSII throughout the season

Despite high irradiance and the occurrence of high temperatures and high VPD in the late summer, the diurnal decreases in F_V/F_M in August 2015 were less pronounced than in the earlier summer months (Fig. 2). The hypothesis of an increased PSII stability was tested by comparing the linear relationship of the F_V/F_M response to environmental constraints in August 2015 with those in other months that year. In

August, we observed a less steep decline in F_V/F_M in relation to increasing T ($p \leq 0.001$, Fig. 7B), and VPD ($p \leq 0.001$, Fig. 7D) compared with the F_V/F_M response in the two previous months. In August, the linear relationship of F_V/F_M to these environmental constraints was similar to that observed in September and October. The F_V/F_M response to SM5 in August 2015 also exhibited a different linear relationship compared with July, with a stronger decrease in relation to decreasing soil moisture ($p \leq 0.001$, Fig. 7C). The response of F_V/F_M to increasing PPFD in August did not differ from the response observed in other months ($p \geq 0.05$, Fig. 7A).

Discussion

Summer was characterized by episodes of low photosynthetic performance due to a combination of environmental constraints. In contrast, high and stable PSII efficiency values were measured in autumn. The discussion here focuses on how meteorological factors influenced the different photosynthetic processes and on which mechanisms were involved in the response of the photosynthetic apparatus in the *L. perenne* population.

L. perenne population showed a down-regulation of PSII photochemical activity in summer under combined stresses

The *L. perenne* population suffered more from PSII photoinhibition in summer, as illustrated by the stronger diurnal F_V/F_M decreases measured in this period (Fig. 2A). Several field studies have reported stronger PSII inhibition in summer for various ecosystems (Fernández-Baco et al. 1998, Arend et al. 2013, Ciccarelli et al. 2016). Reversible diurnal decreases in F_V/F_M have been shown to be related to the cumulative light interception during the day and is described as dynamic photoinhibition (Werner et al. 2001, 2002, Guidi and Calatayud 2014). Photoinhibition is the inactivation of PSII, leading to reduced photosynthetic capacity (Goh et al. 2012), and is generally associated with D1 protein turnover (Aro et al. 1994). It is also described as a photoprotective mechanism that results in the preservation of PSII by diverting light energy from the photosynthetic process (Werner et al. 2001, 2002). The relationship of F_V/F_M with light was confirmed by their comparable diurnal behavior (Fig. 1A,2) and its strong correlation with PPFD (Table 2). Lower F_V/F_M values in summer suggest reduced PSII photochemical efficiency and stronger energy dissipation during this period. The photochemical efficiency of PSII in the *L. perenne* population, however, did not suffer from multiple photoinhibition and was able to recover, as indicated by similar high F_V/F_M values measured in autumn in both years.

The combination of high PPFD in summer with other environmental constraints was associated with a reduction in the overall photosynthetic performance of the *L. perenne* population, shown by the decline in PI_{ABS} under increasingly unfavorable conditions (Table 3, Fig. 5). As indicated in Table 1, the performance index is a multiparametric expression that takes into consideration three important and

independent steps regulating photosynthetic activity: the density of active RC per PSII antenna chlorophyll (RC/ABS); the maximal quantum yield of PSII (F_V/F_M); and the electron transport beyond Q_A (Ψ_{E0}) (Strasser et al. 2000). In our case, PI_{ABS} appeared to be influenced mainly by RC/ABS (data not shown) and F_V/F_M because they exhibited very similar behavior. A reduction in PI_{ABS} could therefore be related to an increase in excitation energy dissipation as well as to an increase in inactive (i.e., non-Q_A reducing) PSII RC. These so-called 'silent RC' are considered a 'heat sink' involved in the down-regulation of the photosynthetic process because they participate in the controlled dissipation of excitation energy (Bussotti et al. 2007, 2011). Large changes in PI_{ABS} have been interpreted in desert scrub species as an ability to down-regulate PSII photochemical activity in order to adapt to environmental changes (van Heerden et al. 2007). In our study, the effects of environmental constraints on photosynthetic activity were usually fully reversible, as illustrated by the recovery of PI_{ABS} in the evening (Fig. 3). This supports the viewpoint of decline in PI_{ABS} as a down-regulation process in response to environmental change and suggests good tolerance in the *L. perenne* population to combined environmental constraints.

Down-regulation of PSII activity is associated with increased efficiency in PSI activity under moderate environmental constraints

The *L. perenne* population demonstrated a higher capacity to reduce the end electron acceptor (i.e., ferredoxin and $NADP^+$) in summer, as indicated by the higher midday ΔV_{IP} values during this period (Fig. 2D). This suggests an up-regulation of the photochemical pathway for the de-excitation of the *L. perenne* population (Pollastrini et al. 2011, Desotgiu et al. 2012). Rapid reduction of the end electron acceptor is typical of 'sun leaves' and expresses a high PSI/PSII ratio (Cascio et al. 2010). Similar photosynthetic behavior was observed among southern European tree species, which exhibited a higher electron transport beyond PSI, as well as lower F_V/F_M and PI_{ABS} values than species from more northern regions (Pollastrini et al. 2016a, b). This behavior was interpreted as acclimatization to higher solar radiation for these species and suggests a rapid delivery of electrons to the final acceptors and then on to the Calvin cycle (photochemical de-excitation). A higher IP phase in rice cultivars was also associated to lower $P700^+$ accumulation (Hamdani et al. 2015). The hypothesis of higher efficiency in electron transport beyond PSI is also supported by the moderate Ψ_{E0} increase, along with ΔV_{IP} increase in conditions of moderate environmental constraints (Table 3), indicating a stimulation in electron transport beyond Q_A.

Strong environmental constraints associated with high temperatures lead to decreased electron transport efficiency beyond Q_A

Stronger environmental constraints, however, could be detrimental to electron transport. Reduced electron transport efficiency (−19% in the Ψ_{E0}) was observed under conditions of strong environmental constraints, but no significant change in ΔV_{IP} was observed (Table 3, Fig. 5). The J phase has been associated with the

redox state of the PQ pool (Tóth et al. 2007a). Decreased Ψ_{E0} values therefore suggest an accumulation of reduced Q_A and PQ pool (Bussotti 2004, Chen et al. 2015). The absence of a significant increase in PSI activity efficiency under conditions of stronger stimulation of the PSII may have been responsible for the slower regeneration of the oxidized form of Q_A and PQ pool. We assumed that reduced in electron transport efficiency beyond Q_A was caused by an imbalance between the electron flow through PSII and the availability of end electron acceptors on the PSI acceptor side. Similar observations have been reported in ozone-fumigated woody species in which events beyond PSI were affected, leading to a reduced ability to manage the electron flux (Cascio et al. 2010, Bussotti et al. 2011). In the case of imbalance between electrons leaving the PSII and those reaching the acceptors beyond PSI, unmanaged electrons (those that come from PSI, but do not reach the end acceptors) can lead to the formation of hydrogen peroxide through the Mehler reaction (Asada 2006) and eventually cause photo-oxidative damage of the cellular content.

A reduction in the efficiency of electron transport between PSII and PSI may play a protective role by limiting the possibility of 'free electrons' beyond the PSI acceptor side. Given that we did not observe a decline in ΔV_{IP}, we assumed that the PSI was not altered by environmental constraints. We therefore suggest that the decline in electron transport was a self-protection strategy because the PSI was not unable to manage the increase in electron flow under conditions of stronger constraints. Our results revealed that electron transport was affected mainly by stress interactions (Fig. 4), particularly during periods of high temperatures such as heat waves (Fig. 2C). A reduction in electron transport efficiency between Q_A and PQ pool was shown to occur at 43°C without alteration of the PSI (Yan et al. 2013). It is possible that interaction between stresses may have reduced the heat threshold above which reduction in electron transport occurs. Taken together, these results indicate the good ability of PSI to manage electron flow except in conditions of strong climatic events when multiple abiotic stresses involving high temperature are combined.

PSII sensitivity to abiotic stress is influenced by sun irradiance and soil moisture

Stronger inhibitions of PSII by heat stress were observed during periods of low soil moisture in the grassland (Fig. 6A). This contrasts with studies that have reported that drought pretreatment benefits PSII thermotolerance (Havaux 1992, Ladjal et al. 2000) due to the accumulation of osmolyte compounds (Oukarroum et al. 2012). These contrasting results might be explained by the need for a period of acclimation to drought conditions that is long enough to allow osmolyte accumulation. High levels of sun irradiance in field conditions might also have influenced plant response to combined water and heat stress. Our results, however, are in accordance with Tozzi *et al.* (2013) who observed a predisposition of PSII to heat stress during a period of drought for Fremont cottonwood grown outdoors.

Exposure to high solar irradiance was also shown to predispose PSII to heat stress (Fig. 6D). Stronger inactivation of PSII under combined stresses might suggest a greater alteration of the thylakoid membrane, as observed for wheat plants (Al-Khatib and Paulsen 1989). Other studies, however, have reported improved PSII stability to heat stress under light exposure due to the accumulation of heat shock proteins (Georgieva et al. 2003) and the activation of the xanthophyll cycle (Buchner et al. 2015). The reversibility in F_V/F_M diurnal declines observed in our study suggests that there was no irreversible damage to the photosynthetic structure. The stronger decline in F_V/F_M values in response to heat stress under high sun irradiance, however, might indicate increased susceptibility to photoinhibition under combined stresses.

In the case of low stomatal aperture (e.g., caused by high VPD or low soil moisture), increased PSII photoinhibition can result from the reduced CO_2 availability for plants continuously exposed to stimulation by high levels of light (Masojidek et al. 1991). Indeed, the limitation of end electron acceptors availability caused by a slowdown in the Calvin cycle can lead to the formation of reactive oxygen species (ROS) beyond the PSI acceptor side (Guidi and Calatayud 2014). A decrease in stomatal conductance might also reduce leaf transpiration, leading to an increase in leaf temperature (Duan et al. 2008, Gago et al. 2015). In our study, however, we did not found increased PSII sensitivity to high levels of light under conditions that promote stomatal closure (Fig 6B, E, F), suggesting that internal CO_2 concentration was not limiting for photosynthesis. The absence of higher PSII sensitivity to increasing VPD under low soil moisture conditions (Fig. 6C) also suggests that *L. perenne* was still able to regulate leaf temperature by transpiration even under conditions of low soil moisture.

L. perenne populations showed an improved PSII tolerance in the late summer

Improved PSII tolerance to abiotic stresses was measured at the end of the summer in 2015, suggesting the acclimatization of the *L. perenne* population in the grassland (Fig. 7). This enhanced PSII stability was evident through better tolerance to low soil moisture, heat stress and high VPD in August than in earlier months. Previous long-term studies conducted on grassland populations did not find any indications of PSII acclimatization after long-term exposure to unfavorable conditions. Gielen et al. (2007), who exposed grassland populations to high temperatures over 3 years, did not observe improved PSII tolerance to midday stress compared with the control. In contrast, the midday depression of F_V/F_M was stronger for populations grown under high air temperature conditions. Different hypotheses might explain this improved PSII tolerance in the *L. perenne* population in August. It is possible that proline and other osmolyte compounds had accumulated in response to the two dry spells in June and July, improving the PSII stability in response to heat stress (De Ronde et al. 2004, Oukarroum et al. 2012). This assumption is supported by experiments showing that cedar seedlings could benefit from drought-induced PSII thermotolerance up to 60 days after re-watering (Ladjal et al. 2000). Improved PSII tolerance in response

to VPD might result from the strong correlation between T and VPD (0.892, $p \leq 0.001$). The stronger decrease in F_V/F_M in response to decreasing soil moisture in July might be explained by the occurrence of a heat wave during this period. The apparent improved PSII tolerance could also result from the selection of genotypes better fitted to the environment (i.e., local adaption). The development of new leaves with different physiological backgrounds might also have contributed to the change in PSII response. These results suggest either the good ability of PSII in the *L. perenne* population to acclimatize and/or an adaptation to local conditions.

Conclusions

Photosynthetic performance of *L. perenne* exhibited a diurnal and seasonal evolution. The strongest photoinhibition of PSII was measured in the summer, when high solar irradiance was combined with other abiotic stresses. Given than the diurnal decreases in ChlF parameters were reversible, the depression of F_V/F_M during this period might indicate increased energy dissipation. The summer was also characterized by stronger PSI activity, reflecting an increased ability in photochemical de-excitation during this period. PSI was unable to increase its activity during strong environmental constraints, however. Strong climatic events led to a reduction in the efficiency in electron transport beyond Q_A. This reduction might, however, contribute to the protection of PSI from oxidative stress by reducing the probability of unmanaged electrons beyond the acceptor side. Low soil moisture had a negligible impact on PSII performance, but was shown to enhance the PSII sensitivity of the *L. perenne* population to heat stress. Increased PSII sensitivity to heat stress was also observed under high sun irradiance. These results illustrate the greater susceptibility of photosynthetic performance under combined stresses. Improved PSII tolerance of heat stress and high VPD was observed in the late summer. Several hypotheses might explain this behavior. Further studies are needed to determine whether or not the improved PSII tolerance measured at the end of the summer was due to improved PSII stability in the *L. perenne* population in response to earlier environmental constraints or the selection of better adapted individuals. In addition, we need to investigate whether or not the photosynthetic performance of different grassland species (e.g., dicots) would respond similarly to these combined climatic events and if an acclimatization of the photosynthetic apparatus is also possible for them. We also need to determine how adjustments in photosynthetic processes influence CO_2 fluxes at the ecosystem level. Experiments are under way to test these hypotheses.

Acknowledgements – We are very grateful to A. Genette and E. Hanon for their useful advice and constructive remarks. We also thank M. Eyletters for constructive discussions and H. Chopin, A. Debacq and F. Wilmus for their technical support. We are grateful to Frederic Collinet and the Calcul et Modélisation Informatique (CAMI) platform of the AGRO-BIO-CHEM department for providing computational resources. The comments by two anonymous reviewers are highly appreciated. This work

was supported by the National Fund for Scientific Research of Belgium (PDR, no. 14614874).

References

Al-Khatib K, Paulsen GM (1989) Enhancement of thermal injury to photosynthesis in wheat plants and thylakoids by high light intensity. Plant Physiol 90: 1041–1048

Arend M, Brem A, Kuster TM, Günthardt-Goerg MS (2013) Seasonal photosynthetic responses of European oaks to drought and elevated daytime temperature. Plant Biol 15: 169–176

Aro EM, McCaffery S, Anderson JM (1994) Recovery from photoinhibition in peas (*Pisum sativum* L.) acclimated to varying growth irradiances (role of D1 protein turnover). Plant Physiol 104: 1033–1041

Asada K (2006) Production and scavenging of reactive oxygen species in chloroplasts and their functions. Plant Physiol 141: 391–396

Boval M, Dixon RM (2012) The importance of grasslands for animal production and other functions: a review on management and methodological progress in the tropics. Animal 6: 748–762

Brestic M, Zivcak M, Kalaji HM, Carpentier R, Allakhverdiev SI (2012) Photosystem II thermostability in situ: environmentally induced acclimation and genotype-specific reactions in *Triticum aestivum* L. Plant Physiol Biochem 57: 93–105

Brunner A, Ammann C, Neftel A, Spirig C (2007) Methanol exchange between grassland and the atmosphere. Biogeosciences 4: 395–410

Buchner O, Stoll M, Karadar M, Kranner I, Neuner G (2015) Application of heat stress in situ demonstrates a protective role of irradiation on photosynthetic performance in alpine plants. Plant Cell Environ 38: 812–826

Bussotti F (2004) Assessment of stress conditions in *Quercus ilex* L. leaves by O–J–I–P chlorophyll a fluorescence analysis. Plant Biosystems 138: 101–109

Bussotti F, Strasser RJ, Schaub M (2007) Photosynthetic behavior of woody species under high ozone exposure probed with the JIP-test: a review. Environ Pollut 147: 430–437

Bussotti F, Desotgiu R, Pollastrini M, Cascio C (2010) The JIP test: a tool to screen the capacity of plant adaptation to climate change. Scand J Forest Res 25: 43–50

Bussotti F, Desotgiu R, Cascio C, Pollastrini M, Gravano E, Gerosa G, Marzuoli R, Nali C, Lorenzini G, Salvatori E, Manes F, Schaub M, Strasser RJ (2011) Ozone stress in woody plants assessed with chlorophyll a fluorescence. A critical reassessment of existing data. Environ Exp Bot 73: 19–30

Bussotti F, Pollastrini M, Holland V, Brüggemann W (2014) Functional traits and adaptive capacity of European forests to climate change. Environ Exp Bot 111: 91–113

Cascio C, Schaub M, Novak K, Desotgiu R, Bussotti F, Strasser RJ (2010) Foliar responses to ozone of *Fagus sylvatica* L. seedlings grown in shaded and in full sunlight conditions. Environ Exp Bot 68:

188–197

Chang J, Ciais P, Viovy N, Vuichard N, Sultan B, Soussana J-F (2015) The greenhouse gas balance of European grasslands. Global Change Biol 21: 3748–3761

Chen S, Kang Y, Zhang M, Wang X, Strasser RJ, Zhou B, Qiang S (2015) Differential sensitivity to the potential bioherbicide tenuazonic acid probed by the JIP-test based on fast chlorophyll fluorescence kinetics. Environ Exp Bot 112: 1–15

Ciccarelli D, Picciarelli P, Bedini G, Sorce C (2016) Mediterranean sea cliff plants: morphological and physiological responses to environmental conditions. J Plant Ecol 9: 153–164

CROSTVOC (2015) The CROSTVOC project – an integrated approach to study the effect of stress on BVOC exchange between agricultural crops and grassland ecosystems and the atmosphere http://hdl.handle.net/2268/178952

Cruz de Carvalho R, Cunha A, Marques da Silva J (2010) Photosynthesis by six Portuguese maize cultivars during drought stress and recovery. Acta Physiol Plant 33: 359–374

D'Ippoliti D, Michelozzi P, Marino C, De'Donato F, Menne B, Katsouyanni K, Kirchmayer U, Analitis A, Medina-Ramón M, Paldy A, Atkinson R, Kovats S, Bisanti L, Schneider A, Lefranc A, Iñiguez C, Perucci CA, Basu R, Samet J, Meehl G, Tebaldi C, Hajat S, Kovats S, Atkinson R, Haines A, Diaz J, Jordán A, Garcia R, Kyselý J, Michelozzi P, De F, Sardon J, Robine J, Cheung S, Roy S Le, Oyen H Van, Griffiths C, Michel J, Herrmann F, Weissekopf M, Anderson H, Foldy S, Michelozzi P, De F, Schwartz J, Michelozzi P, Kirchmayer U, Katsouyanni K, Kalkstein L, Valimont K, O'Neill M, Zanobetti A, Schwartz J, Liang K, Zeger S, Baccini M, Biggeri A, Accetta G, Schwartz J, Dockery D, Hajat S, Armstrong B, Baccini M, Fouillet A, Rey G, Wagner V, Diggle P, Liang K, Zeger S, Chiogna M, Gaetan C, Chiogna M, Gaetan C, Samoli E, Aga E, Touloumi G, Egger M, Smith GD, Altman D, Bouchama A, Tertre A Le, Lefranc A, Eilstein D, Huynen M, Martens P, Schram D, Sprung C, El-Kassimi F, Al-Mashhadani S, Akhtar J, Michelozzi P, Accetta G, Sario M De, Braga A, Zanobetti A, Schwartz J, Hajat S, Armstrong B, Gouveia N, Wilkinson P (2010) The impact of heat waves on mortality in 9 European cities: results from the EuroHEAT project. Environ Health 9: 37

Derks A, Schaven K, Bruce D (2015) Diverse mechanisms for photoprotection in photosynthesis. Dynamic regulation of photosystem II excitation in response to rapid environmental change. Biochim Biophys Acta – Bioenergetics 1847: 468–485

Desotgiu R, Bussotti F, Faoro F, Iriti M, Agati G, Marzuoli R, Gerosa G, Tani C (2010) Early events in *Populus* hybrid and *Fagus sylvatica* leaves exposed to ozone. ScientificWorldJournal 10: 512–527

Desotgiu R, Cascio C, Pollastrini M, Gerosa G, Marzuoli R, Bussotti F (2012) Short and long term photosynthetic adjustments in sun and shade leaves of *Fagus sylvatica* L., investigated by fluorescence transient (FT) analysis. Plant Biosyst 146: 206–216

Duan W, Fan PG, Wang LJ, Li WD, Yan ST, Li SH (2008) Photosynthetic response to low sink demand after fruit removal in relation to photoinhibition and photoprotection in peach trees. Tree Physiol 28: 123–132

Fernández-Baco L, Figueroa ME, Luque T, Davy AJ (1998) Diurnal and seasonal variations in chlorophyll a fluorescence in two mediterranean-grassland species under field conditions. Photosynthetica 35: 535–544

Fox J, Weisberg S, Adler D, Bates D, Baud-Bovy G, Ellison S, Firth D, Friendly M, Gorjanc G, Graves S, Heiberger R, Laboissiere R, Monette G, Duncan M, Nilsson H, Ogle D, Ripley B, Venables W, Winsemius D, Zeileis A, R-Core (2016) Car: Companion to Applied Regression. Available at https://cran.r-project.org/ (accessed 22 July 2016)

Gago J, Douthe C, Coopman RE, Gallego PP, Ribas-Carbo M, Flexas J, Escalona J, Medrano H (2015) UAVs challenge to assess water stress for sustainable agriculture. Agricultural Water Management 153: 9–19

Georgieva K, Tsonev T, Velikova V, Yordanov I (2000) Photosynthetic activity during high temperature treatment of pea plants. J Plant Physiol 157: 169–176

Georgieva K, Fedina I, Maslenkova L, Peeva V (2003) Response of *chlorina* barley mutants to heat stress under low and high light. Funct Plant Biol 30: 515–524

Gielen B, Naudts K, D'Haese D, Lemmens CMHM, De Boeck HJ, Biebaut E, Serneels R, Valcke R, Nijs I, Ceulemans R (2007) Effects of climate warming and species richness on photochemistry of grasslands. Physiol Plant 131: 251–262

Goh C-H, Ko S-M, Koh S, Kim Y-J, Bae H-J (2012) Photosynthesis and environments: photoinhibition and repair mechanisms in plants. J Plant Biol 55: 93–101

Goidts E, van Wesemael B (2007) Regional assessment of soil organic carbon changes under agriculture in southern belgium (1955–2005). Geoderma 141: 341–354

Groemping U, Matthias L (2013) Relaimpo: relative importance of regressors in linear models. Available at https://cran.r-project.org/ (accessed 8 August 2016)

Guidi L, Calatayud A (2014) Non-invasive tools to estimate stress-induced changes in photosynthetic performance in plants inhabiting Mediterranean areas. Environ Exp Bot 103: 42–52

Hamdani S, Qu M, Xin C-P, Li M, Chu C, Govindjee, Zhu X-G (2015) Variations between the photosynthetic properties of elite and landrace Chinese rice cultivars revealed by simultaneous measurements of 820nm transmission signal and chlorophyll a fluorescence induction. J Plant Physiol 177C: 128–138

Hassan IA (2006) Effects of water stress and high temperature on gas exchange and chlorophyll fluorescence in *Triticum aestivum* L. Photosynthetica 44: 312–315

Havaux M (1992) Stress tolerance of photosystem II in vivo: antagonistic effects of water, heat, and photoinhibition stresses. Plant Physiol 100: 424–432

van Heerden PDR, Swanepoel JW, Krüger GHJ (2007) Modulation of photosynthesis by drought in two desert scrub species exhibiting C3-mode CO_2 assimilation. Environ Exp Bot 61: 124–136

Husson F, Josse J, Le S, Mazet J (2016) FactoMineR: multivariate exploratory data analysis and data mining. Available at https://cran.r-project.org/ (accessed 11 July 2016)

Jahns P, Holzwarth AR (2012) The role of the xanthophyll cycle and of lutein in photoprotection of photosystem II. Biochim Biophys Acta – Bioenergetics 1817: 182–193

Janka E, Körner O, Rosenqvist E, Ottosen C-O (2015) Using the quantum yields of photosystem II and the rate of net photosynthesis to monitor high irradiance and temperature stress in chrysanthemum (*Dendranthema grandiflora*). Plant Physiol Biochem 90: 14–22

Jiang Y, Huang B (2001) Physiological responses to heat stress alone or in combination with drought: A comparison between tall fescue and perennial ryegrass. HortScience 36: 682–686

Kalaji HM, Jajoo A, Oukarroum A, Brestic M, Zivcak M, Samborska IA, Cetner MD, Łukasik I, Goltsev V, Ladle RJ (2016) Chlorophyll a fluorescence as a tool to monitor physiological status of plants under abiotic stress conditions. Acta Physiol Plant 38: 102

Ladjal M, Epron D, Ducrey M (2000) Effects of drought preconditioning on thermotolerance of photosystem II and susceptibility of photosynthesis to heat stress in cedar seedlings. Tree Physiol 20: 1235–1241

Luo H-B, Ma L, Xi H-F, Duan W, Li S-H, Loescher W, Wang J-F, Wang L-J (2011) Photosynthetic responses to heat treatments at different temperatures and following recovery in grapevine (*Vitis amurensis* L.) leaves. PLoS One 6: e23033

Masojidek J, Trivedi S, Halshaw L, Alexiou A, Hall DO (1991) The synergistic effect of drought and light stresses in sorghum and pearl millet. Plant Physiol 96: 198–207

Mathur S, Jajoo A, Mehta P, Bharti S (2011) Analysis of elevated temperature-induced inhibition of photosystem II using chlorophyll a fluorescence induction kinetics in wheat leaves (*Triticum aestivum*). Plant Biol 13: 1–6

Maxwell K, Johnson GN (2000) Chlorophyll fluorescence – A practical guide. J Exp Bot 51: 659–668

Menzel U (2015) CCP: significance tests for canonical correlation analysis (CCA). Available at https://cran.r-project.org/ (accessed 25 January 2017)

Mittler R (2006) Abiotic stress, the field environment and stress combination. Trends Plant Sci 11: 15–19

Nash D, Miyao M, Murata N (1985) Heat inactivation of oxygen evolution in photosystem II particles and its acceleration by chloride depletion and exogenous manganese. Biochim Biophys Acta – Bioenergetics 807: 127–133

Oksanen J, Blanchet FG, Friendly M, Kindt R, Legendre P, McGlinn D, Minchin PR, O'Hara RB, Simpson GL, Solymos P, Stevens MHH, Szoecs E, Wagner H (2012) Vegan: community ecology package. Available at https://cran.r-project.org/ (accessed 11 July 2016)

Oukarroum A, Madidi S El, Schansker G, Strasser RJ (2007) Probing the responses of barley cultivars (*Hordeum vulgare* L.) by chlorophyll a fluorescence OLKJIP under drought stress and re-watering. Environ Exp Bot 60: 438–446

Oukarroum A, Schansker G, Strasser RJ (2009) Drought stress effects on photosystem I content and photosystem II thermotolerance analyzed using Chl a fluorescence kinetics in barley varieties differing in their drought tolerance. Physiol Plant 137: 188–199

Oukarroum A, El Madidi S, Strasser RJ (2012) Exogenous glycine betaine and proline play a protective role in heat-stressed barley leaves (*Hordeum vulgare* L.): A chlorophyll a fluorescence study. Plant Biosystems 146: 1037–1043

Pollastrini M, Di Stefano V, Ferretti M, Agati G, Grifoni D, Zipoli G, Orlandini S, Bussotti F (2011) Influence of different light intensity regimes on leaf features of *Vitis vinifera* L. in ultraviolet radiation filtered condition. Environ Exp Bot 73: 108–115

Pollastrini M, Holland V, Brüggemann W, Bussotti F (2016a) Chlorophyll a fluorescence analysis in forests. Annali di Botanica 6: 23–37

Pollastrini M, Holland V, Brüggemann W, Bruelheide H, Dănilă I, Jaroszewicz B, Valladares F, Bussotti F (2016b) Taxonomic and ecological relevance of the chlorophyll a fluorescence signature of tree species in mixed European forests. New Phytol 212: 51–65

Rahbarian R, Khavari-Nejad R, Ganjeali A, Bagheri A, Najafi F (2011) Drought stress effects on photosynthesis, chlorophyll fluorescence and water relations in tolerant and susceptible chickpea (*Cicer arietinum* L.) genotypes. Acta Biologica Cracoviensia Series Botanica 53: 47–56

Redillas MCFR, Strasser RJ, Jeong JS, Kim YS, Kim J-K (2011) The use of JIP test to evaluate drought-tolerance of transgenic rice overexpressing OsNAC10. Plant Biotechnol Rep 5: 169–175

Rizhsky L, Liang H, Mittler R (2002) The combined effect of drought stress and heat shock on gene expression in tobacco. Plant Physiol 130: 1143–1151

De Ronde JA, Cress WA, Krüger GHJ, Strasser RJ, Van Staden J (2004) Photosynthetic response of transgenic soybean plants, containing an *Arabidopsis* P5CR gene, during heat and drought stress. J Plant Physiol 161: 1211–1224

Schansker G, Strasser RJ (2005) Quantification of non-Q_B-reducing centers in leaves using a far-red pre-illumination. Photosynth Res 84: 145–151

Smit MF, Kruger GHJ, van Heerden PDR, Pienaar JJ, Weissflog L, Strasser RJ (2009) Effect of trifluoroacetate, a persistent degradation product of fluorinated hydrocarbons, on C3 and C4 crop

plants. In: Allen JF, Gantt E, Golbeck JH, Osmond B (eds) Photosynthesis. Energy from the sun. 14th International Congress of Photosynthesis Glasgow 2007. Springer, Dordrecht, The Netherlands, pp 623–634

Snider JL, Oosterhuis DM, Collins GD, Pilon C, Fitzsimons TR (2013) Field-acclimated *Gossypium hirsutum* cultivars exhibit genotypic and seasonal differences in photosystem II thermostability. J Plant Physiol 170: 489–496

Strasser R, Srivastava A, Tsimilli-Michael M (2000) The fluorescence transient as a tool to characterize and screen photosynthetic samples. In: Yunnus M, Pathre U, Mohanty P (eds) Probing Photosynthesis: Mechanism, Regulation and Adaptation. Taylor and Francis, London, UK, pp 443–480

Strasser R, Tsimilli-Michael M, Srivastava A (2004) Analysis of the chlorophyll a transient. In: Papageorgiou G, Govindjee (eds) Chlorophyll Fluorescence: A Signature of Photosynthesis. Springer, Dordrecht, The Netherlands, pp 321–362

Tóth SZ, Schansker G, Strasser RJ (2007a) A non-invasive assay of the plastoquinone pool redox state based on the OJIP-transient. Photosynth Res 93: 193–203

Tóth SZ, Schansker G, Garab G, Strasser RJ (2007b) Photosynthetic electron transport activity in heat-treated barley leaves: the role of internal alternative electron donors to photosystem II. Biochim Biophys Acta 1767: 295–305

Tozzi ES, Easlon HM, Richards JH (2013) Interactive effects of water, light and heat stress on photosynthesis in Fremont cottonwood. Plant Cell Environ 36: 1423–1434

Tsimilli-Michael M, Strasser RJ (2008) In vivo assessment of stress impact on plant's vitality: applications in detecting and evaluating the beneficial role of mycorrhization on host plants. In: Mycorrhiza: State of the Art, Genetics and Molecular Biology, Eco-Function, Biotechnology, Eco-Physiology, Structure and Systematics, 3rd ed. Springer, Berlin, Heidelberg, pp 679–703

Werner C, Ryel RJ, Correia O, Beyschlag W (2001) Effects of photoinhibition on whole-plant carbon gain assessed with a photosynthesis model. Plant Cell Environ 24: 27–40

Werner C, Correia O, Beyschlag W (2002) Characteristic patterns of chronic and dynamic photoinhibition of different functional groups in a Mediterranean ecosystem. Funct Plant Biol 29: 999–1011

Wilson RS, Franklin CE (2002) Testing the beneficial acclimation hypothesis. Trends Ecol Evol 17: 66–70

Yan K, Chen P, Shao H, Zhao S, Zhang L, Xu G, Sun J (2012) Responses of photosynthesis and photosystem II to higher temperature and salt stress in sorghum. J Agron Crop Sci 198: 218–225

Yan K, Chen P, Shao H, Shao C, Zhao S, Brestic M (2013) Dissection of photosynthetic electron transport process in sweet sorghum under heat stress. PLoS One 8: e62100

Supporting Information

Additional Supporting Information may be found in the online version of this article:

Table S1. Botanical diversity evaluated on 24 quadrats (0.5 × 0.5 m) during September 2010 and June 2011 at the DTO.

Table S2. Meteorological condition during the two contrasting days.

Table S3. Detailed minimum adequate models used in the calculation of the relative importance of explanatory variables presented in Fig. 5.

Fig. S1. Aerial photography taken on 10 January 2015 of the site of measurement (Dorinne Terrestrial Observatory, DTO) on Google Earth imagery.

Fig. S2. Meteorological conditions over the two studied years.

Edited by J. Flexas

Figure legends

Fig. 1. Environmental conditions prevailing during chlorophyll fluorescence measurements in the 2014 and 2015 study periods. Values for (A) photosynthetic photon flux density (PPFD), (B) air temperature (T), (C) soil moisture (SM5), (D) vapor pressure deficit (VPD) and (E) air ozone concentration (O_3) at 11:00, 13:00, 15:00 and 17:00 h for each day of chlorophyll fluorescence measurements are represented. Grey bars separate the different days of measurements for a better visualization of the diurnal evolution of these parameters. The arrows indicate the first and third day of the heat wave recorded at the DTO. Brackets indicate 31 July 2015 and 13 August 2015.

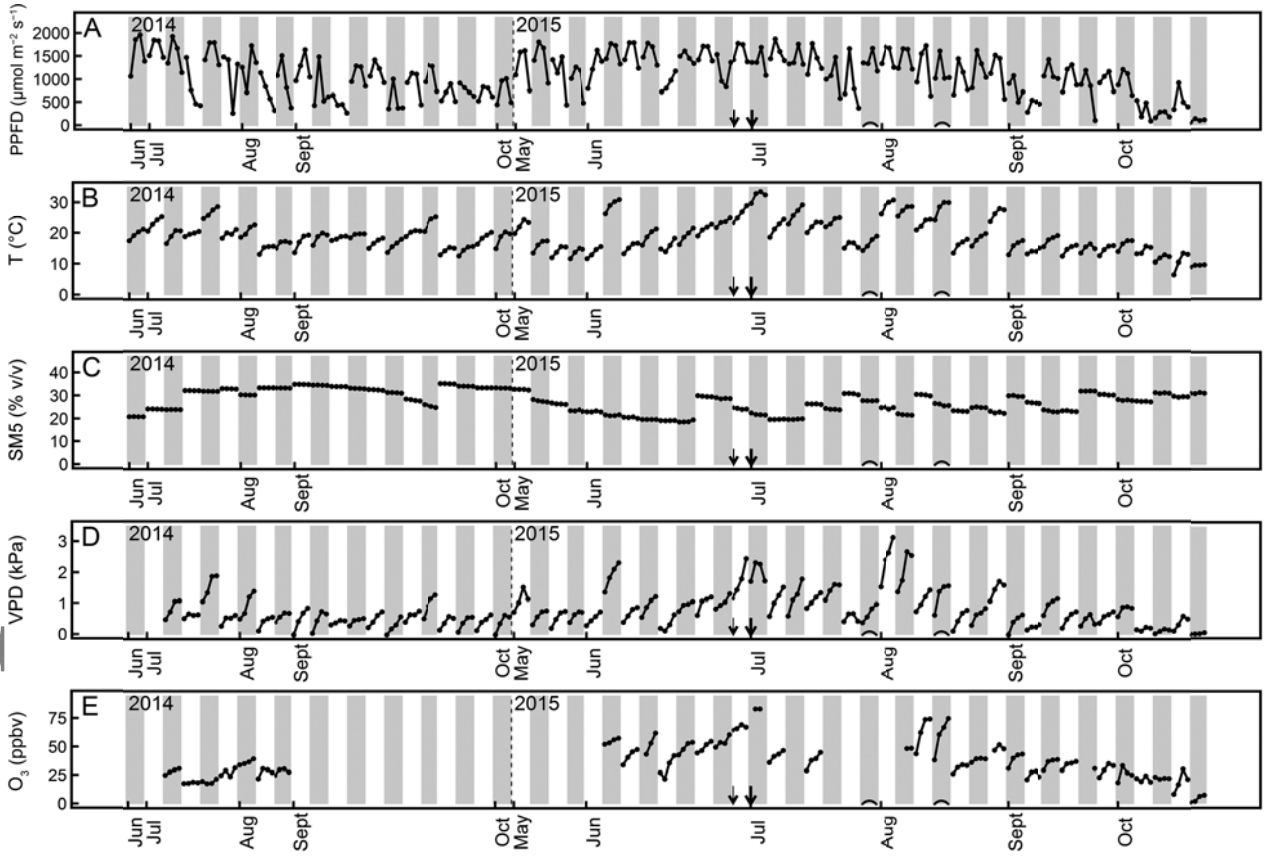

Fig. 2. Evolution of chlorophyll fluorescence (ChlF) parameters (F_V/F_M, PI_{ABS}, Ψ_{E0} and ΔV_{IP}) in the 2014 and 2015 study periods. The average value (n = 21–24) ± SD for each of the four measurement time periods (11:00, 13:00, 15:00 and 17:00 h) is represented for F_V/F_M, PI_{ABS}, Ψ_{E0} and ΔV_{IP} for each measured day. Grey bars separate the different days of measurements for a better visualization of the diurnal evolution of these parameters. The arrows indicate the first and third day of the heat wave recorded at the DTO. Brackets indicate the 31 July 2015 and 13 August 2015.

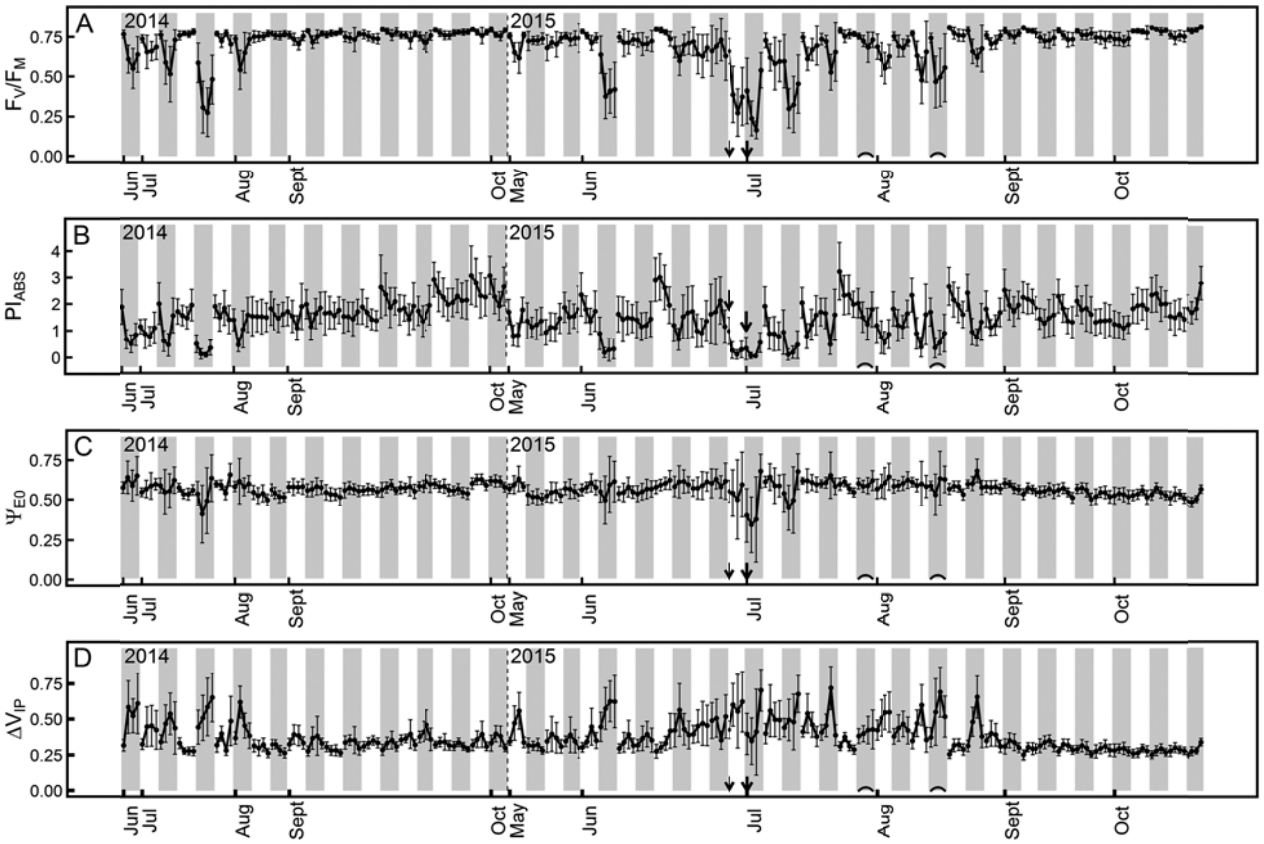

Fig. 3. Diurnal evolution of ChlF parameters over two contrasting days. The average values (n = 24) ± SD for each of the eight sampled time periods (0, 2, 4, 6, 8, 10, 12 and 14 h after sunrise) are represented for the (A) F_V/F_M, (B) PI_{ABS}, (C) Ψ_{E0} and (D) ΔV_{IP} on 31 July 2015 and 13 August 2015. Maximum air temperature was 18.9 and 29.9°C on 31 July 2015 and 13 August 2015, respectively. The photosynthetic photon flux density reached 1669 and 1612 µmol m^{-2} s^{-1} on 31 July 2015 and 13 August 2015, respectively. The maximum vapor pressure deficit was 0.98 and 1.56 kPa on 31 July 2015 and 13 August 2015, respectively. Soil moisture was 27.6±0.1 and 25.9±0.6% on 31 July 2015 and 13 August 2015, respectively. An asterisk indicates a significant difference in ChlF parameters average value between the 31 July 2015 and the 13 August 2015 at a specific sample time periods (GLM, $\alpha = 0.05$). Asterisks *, ** and *** indicate $p \leq 0.05$, $p \leq 0.01$ and $p \leq 0.001$ respectively. For the sake of presentation clarity, the three plots results were pooled because minor significant differences were observed at 0 h after sunrise for PI_{ABS} and Ψ_{E0} only. This did not qualitatively change the results. The grey zone identifies the period when ChlF measurement was routinely performed in the grassland.

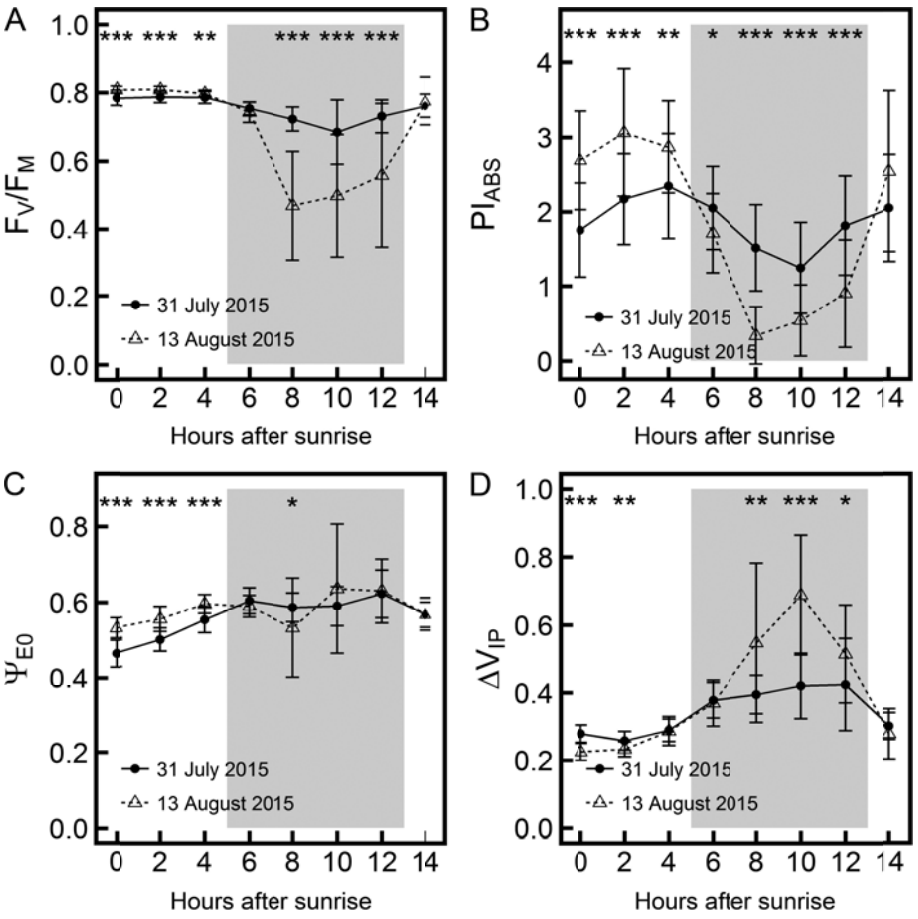

Fig. 4. Relative contribution of the meteorological parameters and their second-order interactions in the models explaining the variability in ChlF parameters. Predictor variables were the air temperature (T), soil moisture (SM5), photosynthetic photon flux density (PPFD) and vapor pressure deficit (VPD). The models explained 80.8, 72.3, 43.3 and 68.4% of the variability in F_V/F_M, PI_{ABS}, Ψ_{E0} and ΔV_{IP}, respectively. Relative humidity and soil moisture were excluded from the model because of their high correlation with vapor pressure deficit (86.55%) and air temperature (84.06%) respectively. The models are detailed in Table S3.

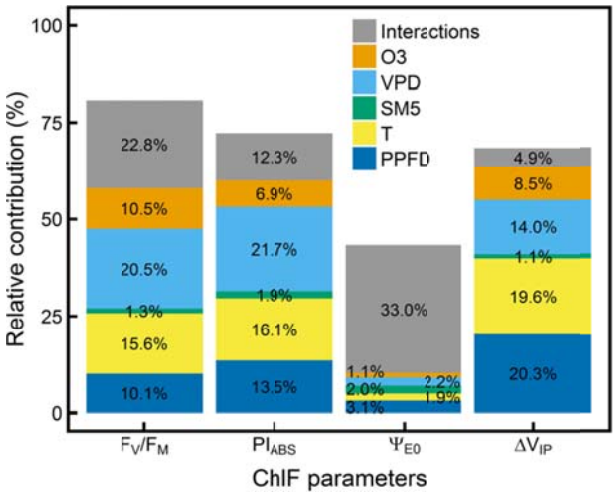

Fig. 5. (A) Canonical correlation analysis (CCA) plot of the distribution of meteorological parameters (left) and ChlF parameters (right) according to the canonical axis 1 (CanAxis1) and 2 (CanAxis). The correlations between the CanAxis1 of the two CCA plot and between the CanAxis2 of the two CCA plots were 86.8% (Wilks' Lambda = 0.158, $F_{24,761}$ = 22.11, *p* value ≤ 0.001) and 48.2% (Wilks' Lambda = 0.641, $F_{15,605}$ = 7.03, *p* value ≤ 0.001), respectively. Meteorological (M1, M2 and M3) and ChlF clusters (C1, C2 and C3) derived from the PCA-clustering were represented in the CCA space to enable the association between the different meteorological conditions and ChlF response groups. See Table 3 for a description of the different group clusters. (B) Correlation circle derived from CCA by combining meteorological parameters (left) and ChlF parameters (right). Meteorological parameters used for the CCA included: photosynthetic photon flux density (PPFD), air temperature (T), vapor pressure deficit (VPD), soil moisture (SM5), relative air humidity (RH) and soil temperature (TS5). Ozone was excluded from the CCA because of the low coverage of these measurements during the measurement period. ChlF parameters used for the CCA included: F_V/F_M, PI_{ABS}, Ψ_{E0} and ΔV_{IP}.

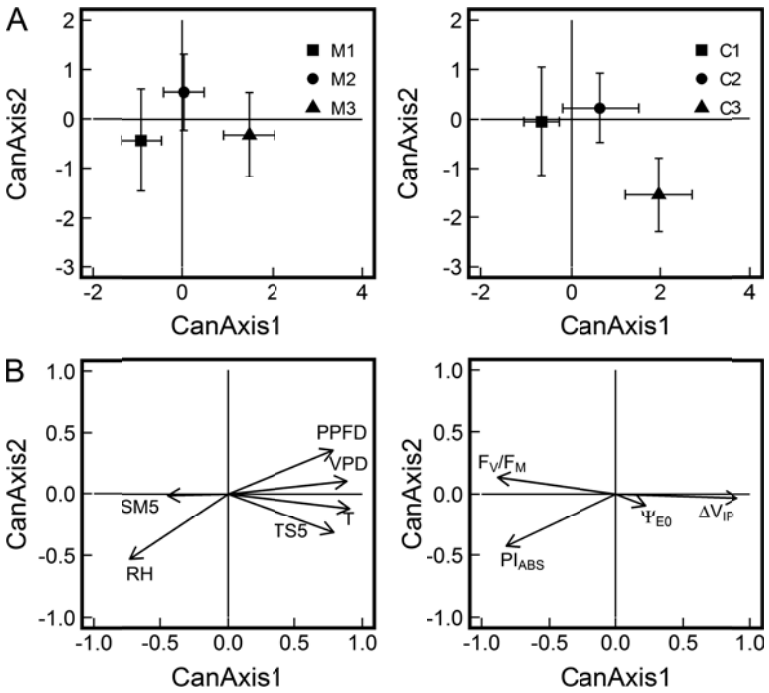

Fig. 6. Response of the maximum quantum yield of PSII (F_V/F_M) (±IC 0.95) to environmental constraints at different soil moisture and sun irradiance levels. Linear regressions of F_V/F_M to (A) increasing air temperature (T), (B) photosynthetic photon flux density (PPFD) and (C) vapor pressure deficit (VPD) for observations performed under three soil moisture conditions in the grassland: wet (SM5 > 30.5% v/v, green line), moderate (25% v/v ≤ SM5 ≤ 27% v/v, blue line) and dry (SM5 < 20.5% v/v, red line). Linear regressions of F_V/F_M response to increasing (D) T, (E) SM5 and (F) VPD for observations performed at three different sun irradiance levels in the grassland: low (PPFD < 1000 µmol m^{-2} s^{-1} , green line), moderate (1000 µmol m^{-2} s^{-1} ≤ PPFD ≤ 1500 µmol m^{-2} s^{-1} , blue line) and high (PPFD > 1500 µmol m^{-2} s^{-1}, red line). Equality of slopes between the different linear regressions was tested by a two-way ANCOVA. Asterisks *, ** and *** indicate $p \leq 0.05$, $p \leq 0.01$ and $p \leq 0.001$, respectively. Different slopes, suggesting a different F_V/F_M response to environmental constraints under different environmental conditions, are reflected by a significant interaction between linear regressions performed under two environmental conditions.

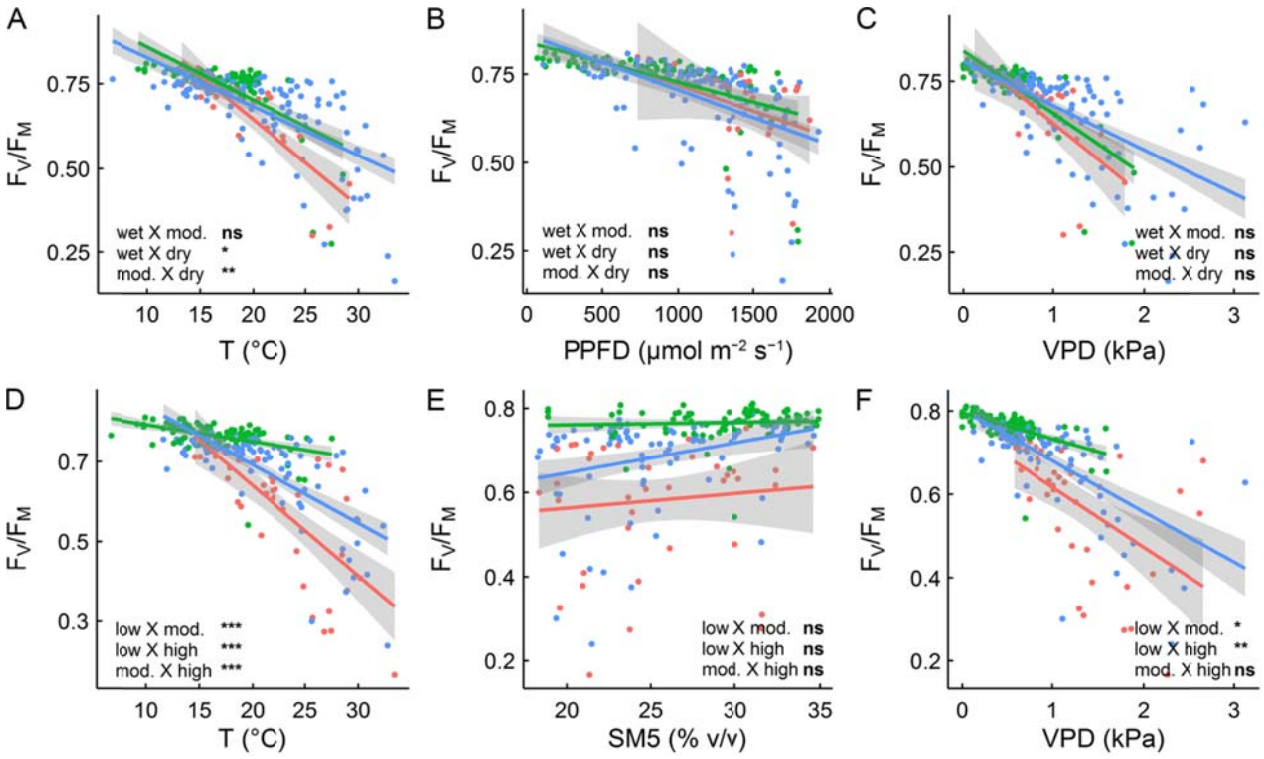

Fig. 7. Response of the maximum quantum yield of PSII (F_V/F_M) (±IC 0.95) to environmental constraints in different months in 2015. Linear regressions of F_V/F_M response to (A) photosynthetic photon flux density (PPFD), (B) increasing air temperature (T), (C) soil moisture (SM5) and (D) vapor pressure deficit (VPD) for observations performed in different months in 2015. The hypothesis of an altered PSII response to environmental constraints in August 2015 compared with other months was tested by a two-way ANCOVA. Asterisks *, ** and *** indicate $p \leq 0.05$, $p \leq 0.01$ and $p \leq 0.001$, respectively. A significant p value indicates a different F_V/F_M response to environmental constraints between August 2015 (reference) and the month under consideration.

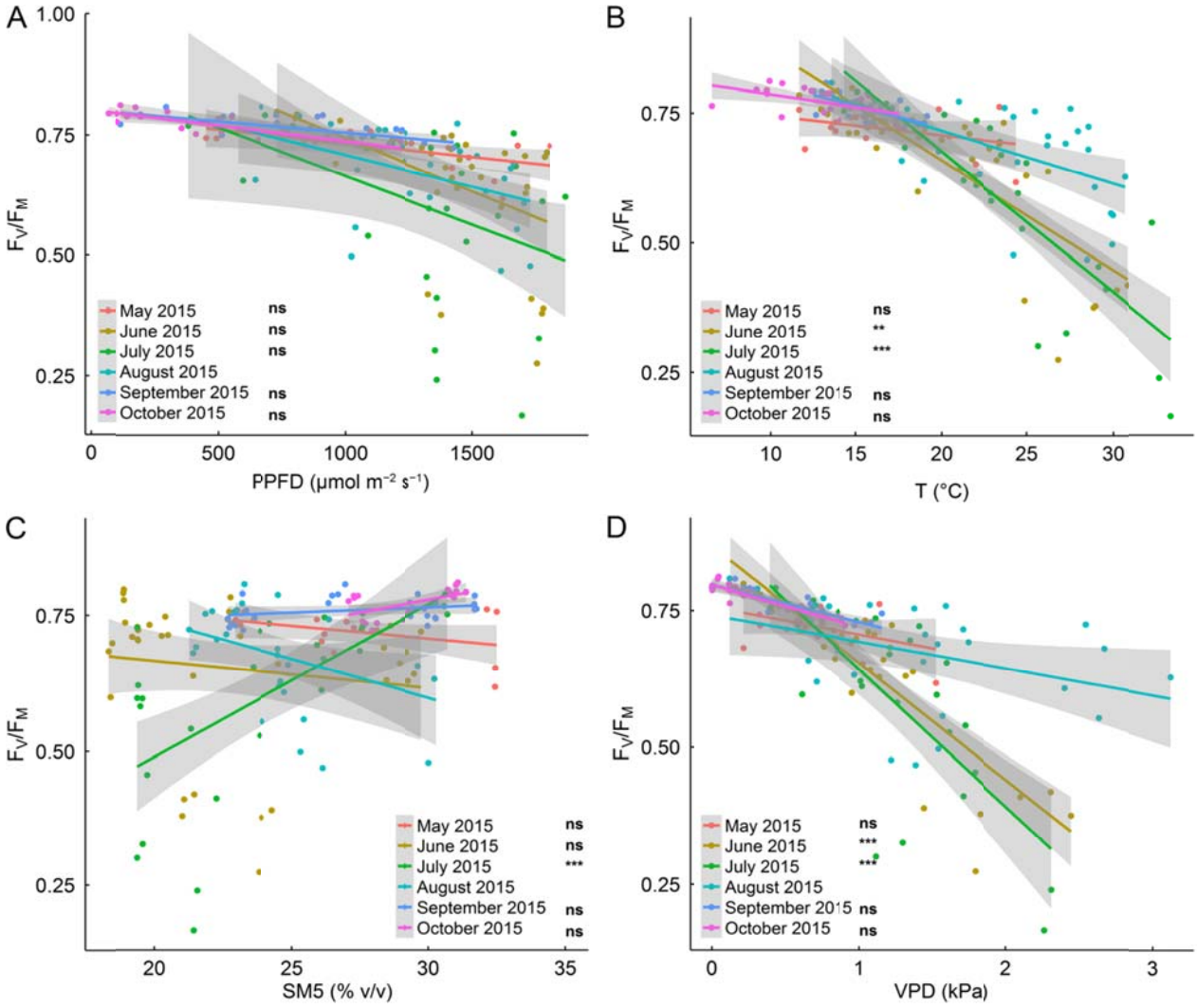

Table 1. Fluorescence parameters.

Parameters	Formula	Description
Technical fluorescence parameters		
$\mathbf{F_t}$		Fluorescence intensity at the time t.
$\mathbf{F_{50}}$		Fluorescence intensity at 50 µs (O-step).
$\mathbf{F_{300}}$		Fluorescence intensity at 300 µs (K-step).
$\mathbf{F_J}$		Fluorescence intensity at 2 ms (J-step).
$\mathbf{F_I}$		Fluorescence intensity at 30 ms (I-step).
$\mathbf{F_M}$		Maximal fluorescence intensity (P-step).
$\mathbf{F_V}$	$F_m - F_{50}$	Maximal variable fluorescence.
$\mathbf{F_V/F_M}$ **(=** $\mathbf{\varphi_{P0}}$**)**	$1 - (F_{50} / F_m)$	Maximum quantum yield of PSII of a dark-adapted leaf. Expresses the probability that an absorbed photon will be trapped by the PSII reaction centre.
JIP-test derived parameters		
$\mathbf{M_0}$	$4.[(F_{300} - F_{50}) / (F_m - F_{50})]$	Approximated initial slope of the fluorescence transient.
$\mathbf{V_t}$	$(F_t - F_{50})/(F_M - F_{50})$	Relative variable fluorescence at the time t.
$\mathbf{V_J}$	$(F_J - F_{50}) / (F_m - F_{50})$	Relative variable fluorescence at 2 ms (J-step).
$\mathbf{V_I}$	$(F_I - F_{50}) / (F_m - F_{50})$	Relative variable fluorescence at 30 ms (I-step).
RC/ABS	$\varphi_{P0} (V_J / M_0)$	Q_A-reducing reaction centres (RC) per PSII antenna Chl.
$\mathbf{\Psi_{E0}}$ **(= J phase)**	$1 - V_J$	The efficiency/probability that a photon trapped by the PSII RC moves an electron into the electron transport chain beyond Q_A.
$\mathbf{\Delta V_{IP}}$ **(= I-P phase)**	$1 - V_I$	The efficiency/probability that a photon trapped by the PSII RC moves an electron into the electron transport chain beyond PSI to reduce the final acceptors of the electron transport chain (i.e., ferredoxin and NADP).
$\mathbf{PI_{ABS}}$	(RC/ABS) $[\varphi_{P0} / (1 - \varphi_{P0})]$ $[\Psi_{E0} / (1 - \Psi_{E0})]$	Performance index (potential) on absorption basis for energy conservation from photons absorbed by PSII to the reduction of intersystem electron acceptors.

Table 2. Correlation values of meteorological parameters (PPFD, photosynthetic photon flux density; T, air temperature; SM5, soil moisture; VPD, vapour pressure deficit; RH, relative air humidity; TS5, temperature of soil; O_3, ozone) with ChlF parameters (F_V/F_M, PI_{ABS}, Ψ_{E0} and ΔV_{IP}). Asterisks *, ** and *** indicate $p \leq 0.05$, $p \leq 0.01$ and $p \leq 0.001$, respectively. ns, non-significant.

	Pearson correlation coefficients			
	F_V/F_M	PI_{ABS}	Ψ_{E0}	ΔV_{IP}
PPFD	−0.564 ***	−0.620 ***	0.164 *	0.622 ***
T	−0.715 ***	−0.632 ***	0.149 *	0.713 ***
SM5	0.350 ***	0.327 ***	−0.052 ns	−0.333 ***
VPD	−0.700 ***	−0.676 ***	0.099 ns	0.682 ***
RH	0.515 ***	0.620 ***	−0.107 ns	−0.543 ***
TS5	−0.564 ***	−0.442 ***	0.267 ***	0.609 ***
O_3	−0.581 ***	−0.488 ***	0.165 ns	0.553 ***

Table 3. Description of the ChlF (C1, C2, C3) and meteorological (M1, M2, M3) group clusters defined by principal component analysis (PCA)-clustering. Mean values ± SD are represented for each cluster. The relative change (Δ%) in the mean with respect to cluster 1 is indicated for each variable in clusters 2 and 3. PPFD, photosynthetic photon flux density (μmol m^{-2} s^{-1}); T, air temperature (°C); SM5, soil moisture (% v/v); VPD, vapour pressure deficit (kPa); RH, relative air humidity (%); TS5, temperature of soil (°C). Ozone was excluded from the PCA-clustering because of the low coverage of these measurements during the measurement period. Different letters indicate significant differences among the clusters (Tukey HSD, $\alpha = 0.05$).

	Variables	Average (± SD) in the different clusters and the percentage change for the C1 or M1 clusters				
		C1 or M1 (□)	C2 or M2 (○)	Δ%	C3 or M3 (Δ)	Δ%
ChlF	F_V/F_M	0.764 ± 0.023 [a]	0.660 ± 0.088 [b]	−13	0.307 ± 0.074 [c]	−60
	PI_{ABS}	1.881 ± 0.467 [a]	1.207 ± 0.514 [b]	−36	0.131 ± 0.093 [c]	−93
	Ψ_{E0}	0.556 ± 0.029 [b]	0.599 ± 0.031 [a]	+8	0.451 ± 0.066 [c]	−19
	ΔV_{IP}	0.303 ± 0.028 [b]	0.456 ± 0.092 [a]	+50	0.491 ± 0.087 [a]	+62
Meteo.	PPFD	674 ± 352 [c]	1242 ± 325 [b]	+84	1432 ± 311 [a]	+112
	T	15.38 ± 3.01 [c]	18.48 ± 3.01 [b]	+20	26.81 ± 3.03 [a]	+74
	SM5	30.90 ± 3.42 [a]	25.91 ± 4.34 [b]	−16	24.29 ± 3.75 [c]	−21
	VPD	0.34 ± 0.20 [c]	0.77 ± 0.22 [b]	126	1.68 ± 0.48 [a]	+394
	RH	81.52 ± 9.96 [a]	64.49 ± 7.29 [b]	−21	53.28 ± 8.41 [c]	−35
	TS5	14.32 ± 2.43 [c]	15.76 ± 3.67 [b]	+10	21.01 ± 2.18 [a]	+47